Materials Research Express

PAPER • **OPEN ACCESS**

Ground-state ferrimagnetism and magneto-caloric effects in Nd_2NiMnO_6

To cite this article: Ranjan Das *et al* 2019 *Mater. Res. Express* **6** 116122

Materials Research Express

PAPER

Ground-state ferrimagnetism and magneto-caloric effects in Nd_2NiMnO_6

Ranjan Das[1], **Premakumar Yanda**[2], **A Sundaresan**[2] and **D D Sarma**[1]

[1] Solid State and Structural Chemistry Unit, Indian Institute of Science, Bengaluru—560012, India
[2] School of Advanced Materials and Chemistry and Physics of Materials Unit, Jawaharlal Nehru Center for Advanced Scientific Research, Jakkur PO, Bengaluru—560064, India

E-mail: sarma@iisc.ac.in

Keywords: double perovskite, magnetism, magnetocaloric effect

OPEN ACCESS

RECEIVED
26 August 2019

REVISED
29 September 2019

ACCEPTED FOR PUBLICATION
15 October 2019

PUBLISHED
25 October 2019

Abstract

Extending our earlier investigation of magnetic properties of Nd_2NiMnO_6, we show that it exhibits a magnetic transition below ~6 K to a ferrimagnetic state. This behavior is interpreted as arising from a long-range ordering of Nd moments antiferromagnetically coupled to the ferromagnetic Ni–Mn ordered moments. Due to the richness of its multiple magnetic transitions and the easily influenced magnetic state by the application of an external magnetic field, established in our earlier study, it has a remarkable inverse magneto-caloric effect (IMCE) at low temperatures ($T < 50$ K) together with a significant conventional magneto-caloric effect (CMCE) at the ferromagnetic ordering temperature ($T_c \sim 200$ K). IMCE and CMCE correspond to the antiferromagnetic arrangement of Nd and Ni–Mn sublattices and ferromagnetic ordering of Ni–Mn sublattices, respectively. Nd_2NiMnO_6 with its second order phase transition follows the universal behavior of $\Delta S_M(T)$; it also shows a power law dependency on the magnetic field as $\Delta S_M \propto H^{\eta}$.

1. Introduction

Double perovskites with the general formula, $A_2BB'O_6$ where, A = rare earth, B and B' = transition metals, with an ordered arrangement of BO_6 and $B'O_6$ are very interesting class of materials because of their large variety of physical properties, such as magnetism, ferroelectricity, magnetoresistance, magneto (dielectric/electric) coupling [1] and magnetocaloric effect (MCE) [2]. All such properties in these compounds depend critically on B/B′-site ordering [3] along with other site and inter-site specific electronic properties, such as the direct and exchange Coulomb interaction, spin–orbit coupling and hopping interaction strengths. Due to these material-specific dependencies, there is an enormous flexibility to tune materials to desired properties by choosing the proper combination of A, B and B′ cations and the extent of ordering [1–5]. As an example, La_2NiMnO_6 undergoes ferromagnetic ordering at around 266 K and, specifically in the presence of Ni/Mn anti-site disorder into a reentrant glassy magnetic state below 150 K [1, 4]. The choice of A = Nd instead of La makes the system richer in terms of the low temperature magnetic phase diagram due to the presence of the magnetic rare-earth ion, Nd. In literature, one can find several studies of magnetic properties of Nd_2NiMnO_6 [5, 6]. It undergoes a ferromagnetic ordering of the Ni–Mn sublattice at around 200 K. While there were conflicting results and interpretations of low temperature magnetic properties, recently it was shown [5] that the diversity in the reported results particularly at an intermediate temperature of about ~150 K arises from different extents of Ni/Mn anti-site ordering, much as in the case of La_2NiMnO_6 [1, 4]. The more interesting, lower temperature magnetic properties were shown to arise from an antiferromagnetic polarization of Nd moments around 50 K due to the internal field of Ni–Mn ferromagnetic sublattice; this results in a prominent and progressive decrease of the magnetization with decreasing temperature below ~50 K [5, 6]. Due to their rich magnetic properties that respond readily to a changing external magnetic field, they are potential candidates for technological applications like magnetic refrigerant technologies.

Magnetic refrigerant technologies work based on the magnetocaloric effect; it arises due to the response of the magnetic sublattice to an external magnetic field [7]. The research in this field has attracted much attention to find new classes of magnetocaloric materials with large changes in the magnetic entropy, ΔS_M, over a wide temperature range upon application of a magnetic field. Magnetic refrigeration is an environment-friendly alternative to vapor-cycle refrigeration, since it does not involve greenhouse gases [8]. Gd and its alloys exhibit large magnetic entropy changes with the application of a magnetic field because of the large spin magnetic moment of Gd [2, 9–11]. Although typically magnetic materials exhibiting first order phase transitions show large ΔS_M (Giant magnetocaloric effect, GMCE), the effect is usually restricted over a narrow range of temperatures near the phase transition [10]. Additionally, due to the presence of hysteresis, they often have low cooling power. To avoid such difficulties, materials exhibiting second order phase transitions are now considered to be better candidates as magnetocaloric materials [2]. Magnetic materials with second order phase transitions do not show thermal hysteresis and they have small $\Delta S_M{}^{pk}$ (maximum change in the entropy), but have significant magnitude over a larger temperature range than GMCE materials, leading to a higher net cooling power. Insulating Nd_2NiMnO_6 with its second order magnetic phase transition and interesting magnetic properties is an obvious candidate as a magnetocaloric material. Here, we show that its magnetocaloric value, ΔS_M, remains significant, though not very large, over a wide temperature range (ΔT_{FWHM}). We also establish the universal behavior of ΔS_M (T), characteristic of a second order phase transition. In addition to this universal behavior of ΔS_M (T), we also show a power law dependency of ΔS_M on the applied magnetic field, $\Delta S_M \propto H^{\eta}$. Interestingly, Nd_2NiMnO_6 exhibits an inverse magnetocaloric effect at the lowest temperature that we suggest as arising from a metamagnetic transition below 10 K. We also identify a transition to a ferrimagnetic state with the total (spin–orbit coupled) moment of Nd^{3+} ordering antiparallel to the Ni–Mn ordered sublattice below ~6 K; this is likely to be the true ground state magnetic structure of Nd_2NiMnO_6.

2. Experimental section

The polycrystalline Nd_2NiMnO_6 sample was synthesized by the conventional sol-gel method [12]. Stoichiometric amount of Nd_2O_3 (preheated at 950 °C) and $MnCO_3$ were dissolved in dilute HNO_3, while $Ni(NO_3)_2$. $6H_2O$ was dissolved in distilled water. These solutions were mixed together, followed by the addition of Citric acid and ethylene glycol as a chelating agent to obtain a gel. The gel was then heated at 170 °C for complete evaporation of the solvent, giving a black powder which was then calcined at 375 °C for decarboxylation. Finally, the powder was pressed into a pellet and heated at 1350 °C for 6 h in the presence of an argon atmosphere. The phase purity of Nd_2NiMnO_6 sample has been confirmed by powder x-ray diffraction (XRD) pattern collected with a Panalytical Philips diffractometer using Cu-K_α as a source of radiation ($\lambda = 1.54056$ Å). The DC magnetization measurements were carried out in a commercial SQUID magnetometer from Quantum Design, USA. Specific heat was measured using Physical Property Measurement System of Quantum Design, USA.

3. Results and discussions

We have shown the diffraction pattern of Nd_2NiMnO_6 together with the Rietveld refinement and the difference plot in figure 1. The refinement yields a monoclinic crystal structure with the space group $P2_1/n$ using MAUD software. The refined lattice parameters are a = 5.4101(2) Å, b = 5.4661(1) Å, c = 7.6617(2) Å, $\alpha = \gamma = 90$ and $\beta = 90.132(3)$ which are in agreement with earlier reports [5, 13] of JCPDS card no. 01-081-9670. We show the dc magnetization of Nd_2NiMnO_6 as a function of temperature in figure 2(a). For the common range of temperatures, this magnetization plot appears similar to the one reported for a highly ordered sample of Nd_2NiMnO_6 [5]. The Nd_2NiMnO_6 sample shows one magnetic transition at ~200 K, associated with Ni–Mn ferromagnetic ordering and a rapid downturn of magnetization with a decreasing temperature below ~50 K, related to a progressive antiparallel alignment of Nd and Ni–Mn sublattice moment [5]. In order to highlight any rapid variation of the magnetization, signaling possible magnetic transitions, we plot the derivative dM/dT as a function of the temperature in figure 2(b). Evidently, the sharp dip in dM/dT at ~200 K reflects the well-known ferromagnetic transition of the Ni–Mn sublattice. Interestingly, we also notice a relatively smaller peak in dM/dT at about 6 K. This low temperature signature of a magnetic transition, shown in an expanded scale as an inset to figure 2(b), is attributed to an ordering of Nd moments in a direction opposite to that of the Ni–Mn ferromagnetically ordered sublattice, representing a ferrimagnetic state. While an antiferromagnetic coupling of the Nd moments to the Ni–Mn moments, arising from a ferromagnetic spin coupling and spin–orbit interactions, was first established in [5], the consequent ferrimagnetic transition was not identified there due to the limited low temperature M(T) data in the earlier study. Figure 2(c) depicts the Curie-Weiss fitting of inverse susceptibility versus temperature plot using equation $\chi = \chi_0 + \frac{C}{T-\theta}$ where χ_0 is the temperature independent

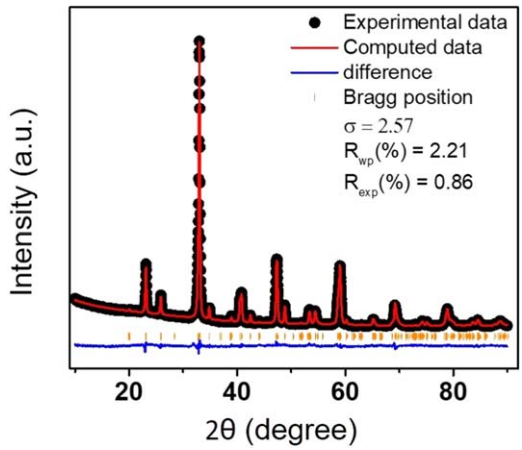

Figure 1. The powder x-ray diffraction (PXRD) pattern of Nd_2NiMnO_6 along with the Rietveld refinement is shown.

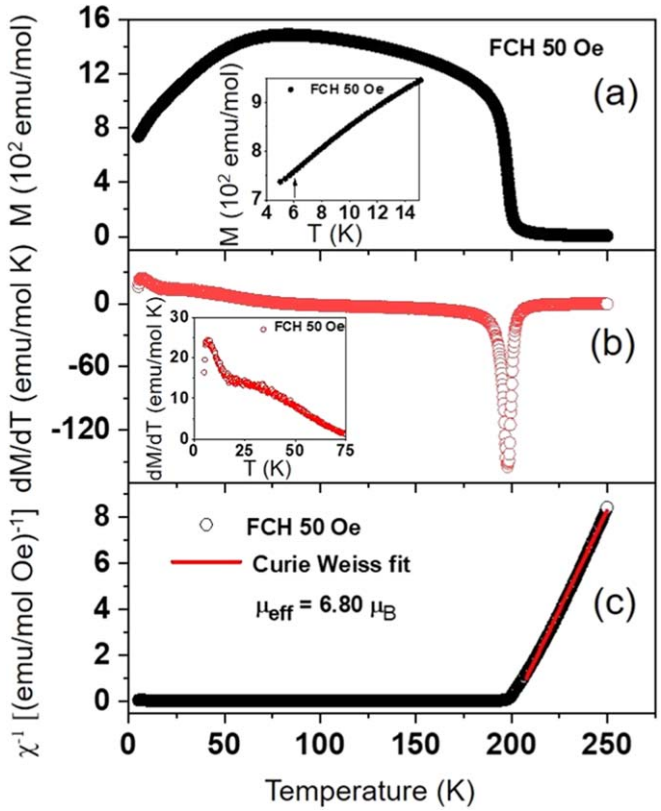

Figure 2. (a) The evolution of magnetization (M) as a function of temperature (T) at 50 Oe magnetic field in field cooled heating (FCH) protocol. The inset in figure 2(a) represents zoomed of M versus T plot at lower temperature. The dM/dT as a function of temperature has been shown in figure 2(b), the sharp dip at ~200 K corresponds to the ferromagnetic Ni–Mn sublattice ordered and the low temperature signature of a magnetic transition, shown in an expanded scale as an inset to figure2(b). Figure 2(c) represents the Curie Weiss fit of inverse susceptibility (χ^{-1}) versus temperature (T).

diamagnetic term, C is the Curie constant and θ is the Curie-Weiss temperature. The experimentally obtained effective moment (μ_{eff}) is 6.80 μ_B/f.u. which is close to the calculated value (7μ_B/f.u.) indicating a high degree of ordering in our sample, since any anti-site disorder between Ni and Mn sites is expected to give rise to a sharp reduction in the effective moment via a strong antiferromagnetic coupling between Ni–O–Ni and Mn–O–Mn superexchange coupled pairs involving the disorder site [5]. The Curie-Weiss temperature, θ, is 201 K, in agreement with the observed T_c.

Thermal evolution of the specific heat (C_p) is depicted in figure 3. The λ- type anomaly in C_p versus T plot at ~200 K confirms the second order ferromagnetic transition. Above 12 K, C_p increases with an increase in the temperature due to the lattice contribution. We note that the downturn in the magnetization for $T \leqslant 50$ K

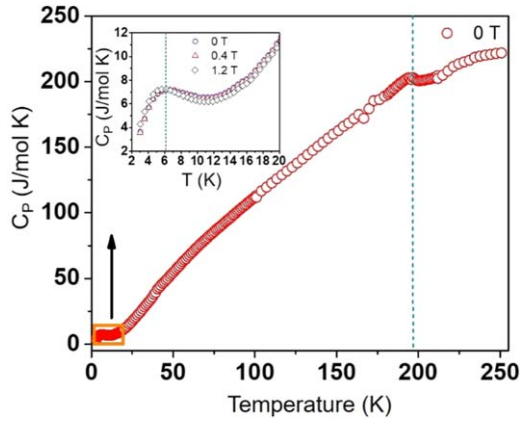

Figure 3. Depicts thermal evolution of specific heat (C_p) at zero magnetic field from 3 K up to 250 K and inset shows the C_p versus T at 0, 0.4 and 1.2 T applied magnetic field for temperature from 20 K down to 3 K.

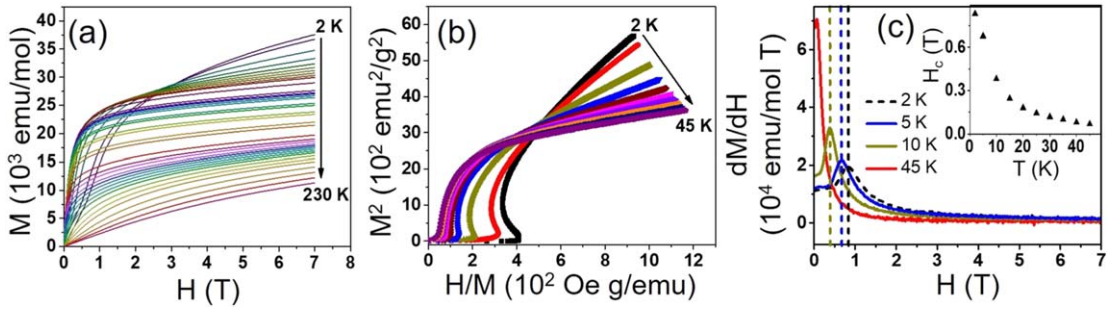

Figure 4. (a) Isothermal magnetization curves at different temperatures 2 K, 5–45 K: $\Delta T = 5$ K, 60 K, 85–105 K: $\Delta T = 5$ K, 120, 125, 140, 145, 160, 165, 180, 185, 188 K, 191–201 K: $\Delta T = 2$ K, 201–210 K: $\Delta T = 3$ K, 210–230 K: $\Delta T = 5$ K. Figure 4(b) Arrott plot (M^2 versus H/M) for temperatures 2 K, 5–45 K: $\Delta T = 5$ K. Figure 4(c) represents the derivative of M with respect to field (H) for a few selected temperatures. Dashed line represents the metamagnetic transitions. Inset of figure 4(c) represents the evolution of critical field (H_c) as a function of temperature.

reported earlier does not reflect itself in any noticeable anomalous change in the C_p(T) plot in the same temperature range; this supports the view expressed in [5] that the change in magnetism in this temperature range is not to be associated with any phase transition. Below 12 K, C_p starts to increase and this is attributed to Nd magnetic contributions. The specific heat anomaly at ~6 K is evidently related to the ordering of Nd ions, as inferred on the basis of the magnetization plot in figure 2.

A series of isothermal magnetization plots are shown in figure 4(a). Below 20 K, the evolution of magnetization with the magnetic field is not monotonic in nature; it also does not show any saturation up to 7 T magnetic field. However, it can be seen that the rise of the magnetization for small applied fields becomes systematically steeper with an increasing temperature. This change leads to the expected behavior above 20 K, where magnetization sharply increases with a very small applied magnetic field and then approaches the saturation at higher fields. These observations make it clear that relatively small magnetic fields are able to perturb the low temperature magnetic state. This is not surprising in view of the weak interaction strengths between the Nd spin and the spin moments of Ni and Mn sites estimated in [5]. This weak magnetic coupling is also evident in the low ordering temperature of 6 K for the ferrimagnetic order. Thus, this sample exhibits a prominent manifestation of metamagnetism in this regime. In order to illustrate this more clearly, we have also shown Arrott plots (M^2 versus H/M) in figure 4(b), showing S-like curvatures for low temperature ($T \leqslant 10$ K) plots. Above 10 K this S-like curvature becomes less prominent. This change of curvature in the Arrott plot over the temperature range also suggests metamagnetic behavior at lower temperatures.

Figure 4(c) shows the dM/dH versus H plots for a few selected temperatures. The critical field (H_c), represented by the position of the maximum of dM/dH plot, appears at ~0.83 T for 2 K. The critical field can be seen to decrease with an increase in temperature of the isothermal curve, vanishing for $T > 45$ K. The existence of the peak in dM/dH as a function of the temperature and the dependence of H_c on T (see inset to figure 4(c)) clearly demonstrate a metamagnetic transition [14, 15].

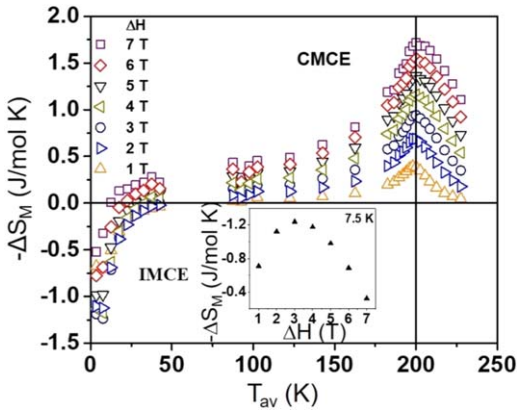

Figure 5. The temperature dependence of isothermal magnetic entropy change calculated from magnetization data for different applied magnetic fields. Inset represents the $-\Delta S_M$ as a function of ΔH for a temperature of 7.5 K.

This low temperature metamagnetic behavior can be understood essentially in terms of the discussion presented in [5] to explain the downturn in magnetization for $T < 50$ K as arising from an antiferromagnetic coupling between Nd spin–orbit coupled moments and Ni–Mn moments. We have shown with the help of figures 2 and 3 that this coupling is responsible for the ferrimagnetic ordering at ~6 K. However, we note that the existence of a peak in dM/dH (H) (figure 4(c)) is not dependent on this ferrimagnetic state. This is clearly illustrated in the inset of figure 4(c), where we plot the position of the peak, H_c, as a function of the temperature. Clearly this peak exists far above the ferrimagnetic transition temperature of 6 K, though it decreases more rapidly above the ordering temperature since the antiferromagnetic exchange coupling strength between Nd and Ni–Mn is weak [5], a sufficiently large applied magnetic field is able to rotate the Nd moments to partially align with the applied magnetic field as shown for $T < 100$ K in [5]. Present results show that a modest applied field is able to also significantly alter the ferrimagnetic order.

We have calculated the isothermal magnetic entropy change from magnetization isotherms by using Maxwell's thermodynamic relation $\Delta S_M(T, \Delta H) = \int_0^H \left(\frac{\partial M(T,H)}{\partial T}\right)_H dH$. As the magnetization measurements were performed at discrete magnetic field changes, we calculate the entropy change numerically [16–18] as

$$-\Delta S_M = \sum_i \frac{(M_i - M_{i+1})}{(T_{i+1} - T_i)} \Delta H_i \quad (1)$$

where, M_i and M_{i+1} are the isothermal magnetization at temperatures T_i and T_{i+1} respectively for a magnetic field change of ΔH_i. In this way, the isothermal magnetic entropy change ($-\Delta S_M$) corresponding to an average temperature $T_{av}\left(T_{av} = \frac{T_i + T_{i+1}}{2}\right)$ is given by the area enclosed between two consecutive magnetic isotherms at T_i and T_{i+1} divided by ΔT ($\Delta T = T_{i+1} - T_i$). We have calculated the isothermal entropy change by using equation (1) and plotted as a function of T_{av} for different magnetic field changes in figure 5. $-\Delta S_M$ changes its sign from negative to positive across a temperature (T_{cross}) ~45 K for 1 T applied magnetic field. T_{cross} decreases with an increase in the applied magnetic field change. The positive value of $-\Delta S_M$ (conventional magnetocaloric effect, CMCE) corresponds to the usual situation where the system favors more ordering (less randomness) on applying an external magnetic field. This is in sharp contrast to the negative value of $-\Delta S_M$ signifying an inverse magnetocaloric effect (IMCE), where the system entropy unexpectedly increases upon applying an external magnetic field. However, from the previous discussion related to figure 2(b), it is easy to understand this phenomenon, since the applied field in this particular case of weak antiferromagnetic exchange coupling between Nd and Ni–Mn is able to perturb the natural alignment of Nd moments significantly. This manifests itself over the temperature range where the induced ordering of Nd moments due to the internal field arising from Ni–Mn ordered lattice is significant, in other words below the temperature (75 K) where dM/dT, in figure 2(b), changes sign.

Reference [5] established that a 3 T external field provides a near complete compensation for the internal field from Ni–Mn ordered moment felt by Nd moments. Thus, the application of this external field allows the maximum entropy associated with Nd moments. Fields higher than this value partially orders Nd moments along the field and any magnetic field lower than 3 T aligns Nd moments antiparallel to Ni–Mn moment. Thus, both an increase and a decrease of the applied field from 3 T leads to a loss in Nd magnetic entropy, explaining the peak in $-\Delta S_M$ observed at 3 T field, as shown in the inset to figure 5.

From figure 5, it is clear that in CMCE region the magnetic entropy change gradually increases and shows maximum value ~1.7 J mol^{-1} K^{-1} at ~200 K (T_c) for magnetic field change of 7 T and above that temperature it

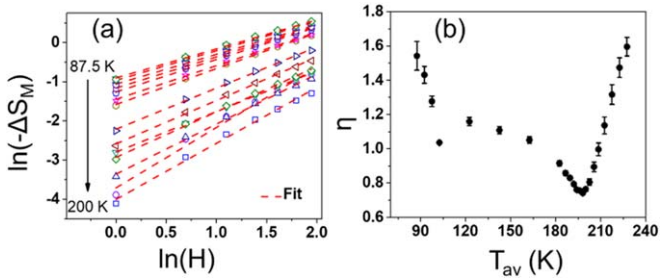

Figure 6. (a) Plot of $\ln(-\Delta S_M)$ versus ln(H) at different temperatures. (87.5 K, 92.5 K, 97.5 K, 102.5 K 122.5 K, 142.5 K, 162.5 K, 182.5 K, 186.5 K, 189.5 K, 192 K, 194 K, 196 K, 198 K, 200 K). The dotted line represents the fitting using the equation $\Delta S_M \propto H^{\eta}$. The evolution of η at three different temperature regions (above T_c, below T_c and at T_c) has been shown in figure 6(b).

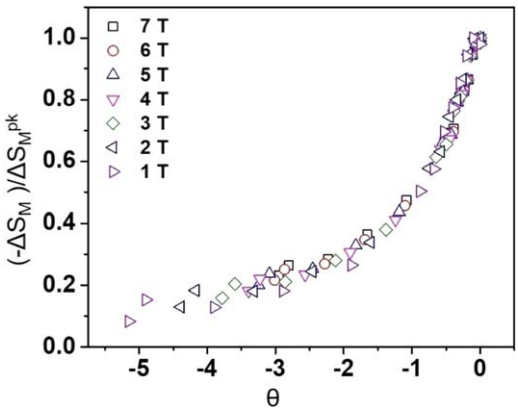

Figure 7. Plot of $(-\Delta S_M/\Delta S_M{}^{pk})$ versus θ, rescaling the temperature axis using equation (2). The magnetic entropy curves for $1\ T \leqslant H \leqslant 7\ T$ merge into one single curve for $T \leqslant T_c$.

decreases slowly. The $-\Delta S_M$ value at 200 K shows a gradual increase with the increase of magnetic field change (see figure 6(a)). The CMCE is due to the presence of the ferromagnetic ordering of Ni–Mn sublattice and it increases with the external magnetic field.

In order to explore whether the magnetic entropy change (ΔS_M) has a power law dependency on the magnetic field, $\Delta S_M \propto H^{\eta}$ we plot $\ln(-\Delta S_M)$ versus ln(H) in figure 6(a). For any given temperature, there is a clear linear dependence, suggesting such a power law. We extract the value of η for different temperatures from linear fits of the data in figure 6(a). Thus, obtained η(T) is plotted in figure 6(b), showing interesting changes. Clearly, η is the lowest at the ferromagnetic transition temperature of ~200 K, rising rapidly with an increasing temperature, approaching the value of 2 expected for non-interacting paramagnetic spins [19]. Below the transition temperature, η is relatively flat for the temperature range of ~100–180 K (figure 6(b)). This corresponds to the relatively flat part of the magnetization as a function of the temperature (see figure 2(a)), where the spontaneous ordering of the spins is expected to lead η to a value of 1 [19]. Indeed, η is in the vicinity of 1 over this temperature range. The rapid change of η observed once again in the lowest temperature regime must be related to the Nd paramagnetic spins whose temperature and field dependent contributions begin to influence the total magnetic moment of the sample significantly. Thus, the change in the magnetic entropy begins to be significantly influenced by the paramagnetic Nd spins at these low temperatures, where η once again approaches the value expected for paramagnetic systems, namely 2 [19, 20]. At $T = T_c$, η has the minimum value of 0.74 ± 0.01. This value is slightly larger than the theoretically predicted value of $\eta = 2/3$ based on a mean field approach [21]. However, similar values of η at the transition temperature has been reported earlier [20, 22, 23].

It has been suggested [19] in recent times that ΔS_M should show a universal scaling behavior as a function of temperature for a second order magnetic transition. Accordingly, we plot $(-\Delta S_M/\Delta S_M{}^{pk})$ versus θ, rescaling the temperature axis as [24–26]

$$\theta = -\frac{(T - T_c)}{(T_{r1} - T_c)} \text{ for } T \leqslant T_c \tag{2}$$

where, T_c (ferromagnetic ordering temperature) is the temperature corresponding to $\Delta S_M{}^{pk}$ and T_{r1} is the temperature corresponding to $\frac{1}{2}\Delta S_M{}^{pk}$. Figure 7 depicts the scaling of ΔS_M for different applied magnetic field

and all the curves converge into one single curve, showing that this system also clearly conforms to the expected behavior.

4. Conclusion

Nd_2NiMnO_6 shows an inverse magneto-caloric effect (IMCE) at a very low temperature along with a conventional magneto-caloric effect (CMCE) at higher temperatures because of the antiparallel alignment of Nd and Ni–Mn sublattice moments in this regime and also due to the presence of spin–orbit coupling of this system. As a consequence, in contrast to Nd_2NiMnO_6, R_2NiMnO_6 where R = La and Gd shows only CMCE throughout the temperature range, since these carry no orbital moment [2, 27] and consequently, has no spin–orbit coupling. We have shown the magnetic entropy change follows the power law dependency of applied magnetic field, $\Delta S_M \propto H^{\eta}$ and η has the minimum value at T_c. The magnetic entropy change also follows the expected universal scaling. In addition, we identify Nd_2NiMnO_6 to have a ground ferrimagnetic state with an ordering temperature of 6 K.

Acknowledgments

The authors thank Department of Science and Technology, Government of India for support. DDS thanks Jamsetji Tata Trust for support.

ORCID iDs

Premakumar Yanda https://orcid.org/0000-0001-9798-1236
A Sundaresan https://orcid.org/0000-0002-1613-3030
D D Sarma https://orcid.org/0000-0001-6433-1069

References

[1] Choudhury D *et al* 2012 *Phys. Rev. Lett.* **108** 127201
[2] Krishna Murthy J, Devi Chandrasekhar K, Mahana S, Topwal D and Venimadhav A 2015 *J. Phys. D: Appl. Phys.* **48** 355001
[3] Sarma D D, Sampathkumaran E V, Ray S, Nagarajan R, Majumdar S, Kumar A, Nalini G and Guru Row T N 2000 *Solid State Commun.* **114** 465–8
[4] Pal S *et al* 2018 *Phys. Rev.* B **97** 165137
[5] Pal S *et al* 2019 *Phys. Rev.* B **100** 045122
[6] Booth R J, Fillman R, Whitaker H, Nag A, Tiwari R M, Ramanujachary K V, Gopalakrishnan J and Lofland S E 2009 *Mater. Res. Bull.* **44** 1559
[7] Pecharsky V K, Gschneidner K A Jr, Pecharsky A O and Tishin A M 2001 *Phys. Rev.* B **64** 144406
[8] Gschneidner K A Jr, Pecharsky V K and Tsokol A O 2005 *Rep. Prog. Phys.* **68** 1479–539
[9] Dey K, Indra A, Majumdar S and Giri S 2017 *J. Mater. Chem.* C **5** 1646
[10] Pecharsky V K and Gschneidner K A Jr 1997 *Phys. Rev. Lett.* **78** 4494
[11] Wagh A A, Suresh K G, Anil Kumar P S and Elizabeth S 2015 *J. Phys. D: Appl. Phys.* **48** 135001
[12] Dass R I, Yan J Q and Goodenough J B 2003 *Phys. Rev.* B **68** 064415
[13] Yadav R and Elizabeth S 2015 *J. Appl. Phys.* **117** 053902
[14] Kakarla D C *et al* 2019 *Phys. Rev.* B **99** 195129
[15] Rai B K *et al* 2018 *Phys. Rev.* X **8** 041047
[16] Zhang X X, Wei H L, Zhang Z Q and Zhang L 2001 *Phys. Rev. Lett.* **87** 157203
[17] Pecharsky V K and Gschneidner K A Jr 1999 *J. Appl. Phys.* **86** 565
[18] Ghara S, Fauth F, Suard E, Rodriquez-Carvajal J and Sundaresan A 2018 *Inorg. Chem.* **57** 12827–35
[19] Franco V, Blázquez J S and Conde A 2006 *Appl. Phys. Lett.* **89** 222512
[20] Pękała M 2010 *J. Appl. Phys.* **108** 113913
[21] Oesterreicher H and Parker F T 1984 *J. Appl. Phys.* **55** 4334
[22] Franco V, Blázquez J S, Millán M, Borrego J M, Conde C F and Conde A 2007 *J. Appl. Phys.* **101** 09C503
[23] Li Z, Zhang L, Zhang X, Li Y, Zhao Q, Zhao T and Shen B 2017 *J. Phys. D: Appl. Phys.* **50** 015002
[24] Franco V and Conde A 2010 *Int. J. Refrig* **33** 465–73
[25] Bonilla C M, Herrero-Albillos J, Bartolomé F, García L M, Parra-Borderías M and Franco V 2010 *Phys. Rev.* B **81** 224424
[26] Bonilla C M, Bartolomé F, García L M, Parra-Borderías M, Herrero-Albillos J and Franco V 2010 *J. Appl. Phys.* **107** 09E131
[27] Matte D, Lafontaine M, Ouellet A, Balli M and Fournier P 2018 *Phys. Rev. Appl.* **9** 054042